Pressure-induced quantum phase transitions in a YbB_{6} single crystal

Yazhou Zhou, Dae-Jeong Kim, Priscila Ferrari Silveira Rosa, Qi Wu, Jing Guo, Shan Zhang, Zhe Wang, Defen Kang, Wei Yi, Yanchun Li, Xiaodong Li, Jing Liu, Peiquan Duan, Ming Zi, Xiangjun Wei, Zheng Jiang, Yuying Huang, Yi-feng Yang, Zachary Fisk, Liling Sun, and Zhongxian Zhao

Phys. Rev. B **92**, 241118 — Published 29 December 2015

DOI: 10.1103/PhysRevB.92.241118

Pressure-induced quantum phase transitions in YbB_6single crystal

Yazhou Zhou[1], Dae-Jeong Kim[2], Priscila Ferrari Silveira Rosa [2], Qi Wu[1], Jing Guo[1], Shan Zhang[1], Zhe Wang[1], Defen Kang[1],Wei Yi[1],Yanchun Li[3], Xiaodong Li[3], Jing Liu[3], Peiquan Duan[4], Ming Zi[4], Xiangjun Wei[4], Zheng Jiang[4], Yuying Huang[4], Yi-feng Yang[1,5], Zachary Fisk[2], Liling Sun[1,5]† & Zhongxian Zhao[1,5]

[1]*Institute of Physics and Beijing National Laboratory for Condensed Matter Physics, ChineseAcademy of Sciences, Beijing 100190, China*

[2]*Department of Physics and Astronomy, University of California, Irvine, CA92697, USA*

[3]*Institute of High Energy Physics, ChineseAcademy of Sciences, Beijing 100049, China*

[4]*Shanghai Synchrotron Radiation Facilities, Shanghai Institute of Applied Physics, ChineseAcademy of Sciences, Shanghai 201204, China*

[5]*Collaborative InnovationCenter of Quantum Matter, Beijing 100190, China*

We report the first observation of two pressure-induced quantum phase transitions in YbB_6 single crystal, *i.e.* from a topologically trivial semiconductor to an intermediate semimetal and then from the semimetal to a possible topologically non-trivial high-pressure gapped phase, through *in-situ* high pressure transport and synchrotron X-ray diffraction measurements.Our high pressure absorption results reveal that the mixed valence state in pressurized YbB_6 above 15 GPa plays an important role in the formation of the high-pressure state with a re-opened gap. These high pressure results may be helpful for shedding light on the intriguing relation between the topology and 4*f* electrons in the rare earth hexaborides.

PACS numbers: 71.55.Ak, 74.62.Fj, 71.30.+h

In recent years, topological insulators (TIs) attract intensive interests due to their non-trivial properties of coexisting insulating bulk and topologically protected conducting surface [1-5]. Such exotic electronic states have been observed in the compounds of Bi_2Se_3, Bi_2Te_3 and HgTe [6-10]. A new advance in the field is the possible existence of such a topological state in the rare-earth hexaborides SmB_6 and YbB_6 [11-17]. Because of containing *f*-electrons, these hexaborides may exhibit a variety of exotic electronic correlation effects. In particular, they may host the novel topological electronic states that are different from the usual TIs without *f*-electrons [11,15,18,19]. These hexaborides are thus expected to bridge the physics between correlated electron material and topological insulator. As a candidate material for the new class of TIs, ambient-pressure SmB_6 undergoes a transition from a poor metal at room temperature to a Kondo insulator with residual conductance at low temperature [14,20,21]. Theoretical calculations point out that the low temperature residual conductance in SmB_6 is originated from the non-trivial conducting surface state due to the hybridization between *d*-orbitals and *f*-orbitals of Sm ions [22]. Soon after, these predictions have been identified by many experimental measurements [12,13,17,20,21,23-36]. These results support that SmB_6 is a topological Kondo insulator (TKI). For YbB_6, it crystallizes in the same structure as that of SmB_6, but presents very different electronic structures due to that Yb has a fully filled 4*f* shell while Sm has nearly half-filled 4*f*-shell. Some results from angle resolved photoemission spectroscopy (ARPES) measurements on the ambient-pressure YbB_6 propose that it is a topological insulator [16,37,38]. While, other ARPES

measurements argue that the YbB_6 is not a TI [39,40]. To shed light on the nature of the electronic state in ambient-pressure YbB_6 and explore its potential new quantum phenomena, we performed high pressure resistance, Hall coefficient, X-ray diffraction and X-ray absorption measurements on this hexaboride.

High quality single crystals of YbB_6 were grown by the Al flux method, as described in Ref.[21]. Pressure was generated by a diamond anvil cell (DAC) with two opposing anvils sitting on the Be-Cu supporting plates. Diamond anvils with 400 μm and 300 μm flats, and nonmagnetic rhenium gaskets with 200 μm and 100 μm diameter holesrespectively, were employed for different runs of the high-pressure studies. The four-probe method was applied on the (001) facet of single crystal YbB_6 for all high pressure transport measurements. To keep the sample in a quasi-hydrostatic pressure environment, NaCl powder was employed as the pressure medium for the high-pressure resistance, magnetoresistance and Hall effect measurements. High pressure X-ray diffraction (XRD) and X-ray absorption spectroscopy (XAS) experiments were performed at beam line 4W2 at the Beijing Synchrotron Radiation Facility and at beamline 14W1 at the Shanghai Synchrotron Radiation Facility, respectively. Diamonds with low birefringence were selected for the experiments. A monochromatic X-ray beam with a wavelength of 0.6199 Å was adopted for all XRD measurements. To maintain the sample in a hydrostatic pressure environment, silicon oil was used as pressure medium in the high-pressure XRD and XAS measurements. Pressure was determined by the ruby fluorescence method [41].

Figure 1 shows the results of high-pressure resistance measurements for a single

crystalline sample of YbB_6. Although the sample exhibits metallic behavior in the temperature range 50-300 K at 0.9 GPa, at lower temperature an insulating behavior sets in, as manifested by a small upturn below 50 K (Fig.1a). This upturn is observed in three independent runs' measurements on samples obtained from different batches, consistent with its ambient-pressure behavior (Fig.S1 of Supplementary Information). Upon increasing pressure, the upturn is suppressed dramatically (Fig.1a) andeventually goes away at ~ 10 GPa (Fig. 1b). Subsequently, metallic resistance behavior over entiretemperature range is observed in the pressure range 10.5-14.2 GPa (Fig.1b), reflecting the closure of the semiconducting gap in the bulk and the conversion from its semiconducting state into a metallic state. Upon further increasing pressure, interestingly, a resistance upturn presents at 15.2 GPa and becomes pronounced at higher pressures (Fig.1b and 1c). At 19.8 GPa, an apparent resistance plateau is observed at low temperatures (inset of Fig.1c), similar to what has been seen in the SmB_6 [21].The onset temperature (T*) of the plateau shifts to higher temperature upon increasing pressure (inset of Fig.1c and Fig.1d). Since the lowest temperature of our instrument is 4 K, we cannot detect the T* (it should be below 4 K) for the sample subjected to pressures ranging from 15 GPa to 19 GPa. Extrapolation of the obtained T* down to lower pressure gives a critical pressure point at ~15 GPa (Fig.1d), where the gap is coincidently closed. To determine the critical pressures for these two phase transitions, we plot the pressure dependence of the resistance at different temperatures (Fig.1e). It is seen that the resistance at all temperatures remains nearly unchanged between 10-15 GPa, butshows very different trends below

10 GPa and above 15 GPa, giving rise to the two critical pressures:P_{C1} (~10 GPa) which separates the semiconducting state and the metallic state, and P_{C2} (~15 GPa) which separates the metallic state and the high pressure-induce state with a resistance upturn.

To further characterize these pressure-induced changes in YbB_6, we performed high pressure Hall effect measurements. The Hall coefficientR_H measured at 4 K is plotted as a function of pressure in Fig.1f. The R_H displays negative value over the entire pressure range, indicating that electron carriers are dominant in YbB_6. We find that below ~4 GPa the absolute value of R_H decreases rapidly with increasing pressure. This remarkable decrease corresponds to the dramatic reduction of the resistance (Fig.1e). However, for pressures ranging from 10 GPa to 15 GPa, the R_H barely changes, which may be attributed to the balance between electron and hole carrier population, demonstrating that the intermediate phase is in a semimetallic state[42]. Significantly, an enhancing trend of R_H upon increasing pressure is observed above 15 GPa. This increase in R_H is consistent with theobserved upturn behavior of the resistance (Fig.1b and 1c).

To clarify whether the physical origin of the gap closing and re-opening observed in the pressurized YbB_6 is related to a structural phase transition, we conducted high pressure X-ray diffraction experiments for YbB_6 at beamline 4W2 at the Beijing Synchrotron Radiation Facility. We find that increasing pressure consistently pushes all Bragg peaks to a larger 2θ angle, but no new peaks appear up to 31.2 GPa (Fig.2a). The lattice parameter exhibits linear pressure-dependence and the plot of pressure

dependent volume shows noobvious discontinuity (Fig.2b and 2c). Earlier studies by Sidorov*el al* [42] also found an exponential decrease in resistivity within ~ 5 GPa and no structural phase transition detected by XRD measurements up to 8 GPa, in good agreement with our low pressure results. These results rule out the possibility of pressure-induced structural phase transition in YbB_6 and indicate that the closing and re-opening of the activation energy gap are electronic origin.

The low pressure range transport behavior of YbB_6 provides an important understanding of its ambient pressure electronic structure, a keyissue for its topological nature. The combined results of the pressure-induced decline in resistivity approaching to 10 GPa, the suppression of activation energy and constant Hall coefficient in the pressure range 10-15 GPa provide the consistent evidence for that the intermediate metallic state is a *p-d* overlapped semimetallic state, and thus this semimetallic state should be evolved from a *p-d* gapped semiconducting state. This evolution has been theoretically explained and the ambient pressure state has been identified by ARPES measurements very recently [40].

Figure 3a plots *dR/dT* curves measured in the temperature range 4-300 K for all pressurized samples. The activation energy (ε_a) as a function of pressure is estimated using the equation$R(T) = 1/[R_S^{-1} + R_B^{-1} exp^{-\varepsilon_\alpha/2k_BT}]$, where the first component is the resistance from the surface contributionand the second one from the bulk contribution.We find a good fit to the experimental data in the two gaped regimes (Fig. S2 of Supplementary Information). The solid dots in Fig.3a are the extracted activation energy (ε_a) of the sample subjected to different pressures. It is seen that, at

the base temperature, the phase diagram contains three distinct regimes. In the left regime, ε_a is reduced with increasing pressure and approaches zero at P_{C1} (~ 10 GPa), demonstrating that the host sample undergoes a transition from a topological trial semiconducting (TT-S) state with a positive *dR/dT*in the high temperature range and a negative *dR/dT* in the low temperature range to a semimetallic (SM) state (the middle regime). On further increasing pressure above Pc_2, the sample moves into a novel high-pressure state with a re-opened gap (the right regime).

Intriguingly, the behavior of the low-temperature resistance plateau in pressurized YbB_6 above Pc_2 is very similar to that of ambient-pressure SmB_6 (Fig. 1c). It is hence natural to ask whether this high-pressure gapped state is topologically non-trivial. To know the answer, we applied a magnetic field of 7 Tesla (T) on the sample at given pressures and findan enhancement of its resistance in the whole temperature range for the pressures ranging from 16.3 GPa to 23.9 GPa (Fig.3b-d). The similar positive magnetoresistance behaviors have been found in TKI SmB_6 under the magnetic field below ~ 4.5 T, which is taken as a signature of the surface state protected by a time reversal symmetry [21].

Another striking feature of SmB_6 is its mixed valence state. For the valence state of YbB_6, we note that previous ARPES measurements and X-ray photoelectron experimentsat ambient pressure have established that the divalent Yb component is dominant in the bulk YbB_6 [43]. To know the pressure dependent valence state of Yb ions and especially clarify whether the high-pressure gapped phase is in a mixed valence state, we performed high-pressure X-ray absorption measurements at

beamline 14W1 at Shanghai Synchrotron Radiation Facilities. Representative L_{III}-edge X-ray absorption spectra (XAS) of YbB_6 collected at different pressures are presented in Fig.4a. In the pressure range investigated, the Yb^{2+} peak is clearly seen at 8939.8eV but no visible Yb^{3+} peak is observed at higher energy. Instead, a dip is found at 8946.3eV where the Yb^{3+} peak usually appears. Significantly, we find that the intensity of Yb^{2+} peak decreases upon increasing pressure, while the dip isgraduallyfilled up. A careful analysis on the extended X-ray absorption spectra for the sample indicates that the pressure-induced reduction of the dip should be attributed to the growth of the Yb^{3+} component (Fig.S3 of Supplementary Information). As is shown in Fig. 4b, the absorption spectra collected at ambient pressure and 28.2 GPa clearly demonstrate how the pressure-induced enhancement of the Yb^{3+} spectral weight compensates the observed ambient-pressure dip. Taking the mean valence of Yb at ambient pressure as v=2, the pressure dependence of v (Fig.4c) can be deduced from the relative intensities of the Yb^{2+} and Yb^{3+} components. We find that the $v$remains nearly unchanged below 10 GPa, whereas it increases remarkably at pressure greater than 15 GPa where YbB_6 enters the high-pressure gapped state. These results reveal the sensitive nature of the bulk valence in YbB_6, for which Sidorov*et al* [42]hypothesized the possible mixed valence state at high pressure with the recommendation of L_{III}-edge XAS measurements– now performed here 24 years later. Our high-pressure X-ray absorption measurements confirmed the bulk divalency in YbB_6 at (or near) ambient pressure, and significantly discovered the onset of mixed–valency at high pressure.

The achieved results, including pressure-induce gap closing and re-opening, resistance plateau, positive magnetronresistance effect and the mixed valence state, inspire us to propose that this high-pressure gapped state in YbB_6 may be topologically non-trivial. Therefore, we denote the pressure-induced gapped state as a topologically non-trivial high pressure phase (TNT-HP phase) in the phase diagram (Fig.3a).The theoretical studies of Ref.40 on the electronic structure of pressurized YbB_6 propose that the pressurized YbB_6 above 15 GPa may be a partially-gapped semimetal. This interesting high-pressure gapped phase with topologically non-trivial features deserves further investigations.

In conclusion, we find two pressure-induced quantum phase transitions in YbB_6, from the ambient-pressure *p-d* gapped semiconducting state to the intermediate semimetallic state and then from the semimetallic state to a possible topologically non-trivial gapped state, through *in-situ* high pressure transport and synchrotron X-ray diffraction measurements. Our results demonstrate that the pressure-induced semimetallic state is a pathway connecting the ambient-pressure semiconducting state and the high-pressure gapped state. Significantly, our high pressure absorption results reveal that the mixed valence state in pressurized YbB_6 above 15 GPa plays an important role in the development of the high-pressure gapped state.

References

[1] L. Fu, C. Kane, and E. Mele, Phys. Rev. Lett. **98**, 106803 (2007).

[2] J. Moore and L. Balents, Phys. Rev. B **75**, 121306 (2007).

[3] X.-L. Qi, T. Hughes, and S.-C. Zhang, Phys. Rev. B **78**, 195424 (2008).

[4] M. Z. Hasan and C. L. Kane, Rev. Mod. Phys. **82**, 3045 (2010).

[5] X. L. Qi and S. C. Zhang, Rev. Mod. Phys. **83**, 1057 (2011).

[6] M. Konig, S. Wiedmann, C. Brune, A. Roth, H. Buhmann, L. W. Molenkamp, X. L. Qi, and S. C. Zhang, Science **318**, 766 (2007).

[7] Y. L. Chen, J. G. Analytis, J. H. Chu, Z. K. Liu, S. K. Mo, X. L. Qi, H. J. Zhang, D. H. Lu, X. Dai, Z. Fang, S. C. Zhang, I. R. Fisher, Z. Hussain, and Z. X. Shen, Science **325**, 178 (2009).

[8] H. J. Zhang, C. X. Liu, X. L. Qi, X. Dai, Z. Fang, and S. C. Zhang, Nat. Phys. **5**, 438 (2009).

[9] D.-X. Qu, Y. S. Hor, J. Xiong, R. J. Cava, and N. P. Ong, Science **329**, 821 (2010).

[10] J. S. Zhang, C. Z. Chang, P. Z. Tang, Z. C. Zhang, X. Feng, K. Li, L. L. Wang, X. Chen, C. X. Liu, W. H. Duan, K. He, Q. K. Xue, X. C. Ma, and Y. Y. Wang, Science **339**, 1582 (2013).

[11] F. Lu, J. Zhao, H. Weng, Z. Fang, and X. Dai, Phys. Rev. Lett. **110**, 096401 (2013).

[12] M. Neupane, N. Alidoust, S. Y. Xu, T. Kondo, Y. Ishida, D. J. Kim, C. Liu, I. Belopolski, Y. J. Jo, T. R. Chang, H. T. Jeng, T. Durakiewicz, L. Balicas, H. Lin, A. Bansil, S. Shin, Z. Fisk, and M. Z. Hasan, Nat. Commun. **4**, 7 (2013).

[13] C.-H. Min, P. Lutz, S. Fiedler, B. Y. Kang, B. K. Cho, H. D. Kim, H. Bentmann, and F. Reinert, Phys. Rev. Lett. **112**, 226402 (2014).

[14] W. A. Phelan, S. M. Koohpayeh, P. Cottingham, J. W. Freeland, J. C. Leiner, C. L. Broholm, and T. M. McQueen, Phys. Rev. X **4**, 031012 (2014).

[15] H. M. Weng, J. Z. Zhao, Z. J. Wang, Z. Fang, and X. Dai, Phys. Rev. Lett. **112**, 5, 016403 (2014).

[16] M. Xia, J. Jiang, Z. R. Ye, Y. H. Wang, Y. Zhang, S. D. Chen, X. H. Niu, D. F. Xu, F. Chen, X. H. Chen, B. P. Xie, T. Zhang, and D. L. Feng, Sci. Rep. **4**, 6, 5999 (2014).

[17] N. Xu, P. K. Biswas, J. H. Dil, R. S. Dhaka, G. Landolt, S. Muff, C. E. Matt, X. Shi, N. C. Plumb, M. Radović, E. Pomjakushina, K. Conder, A. Amato, S. V. Borisenko, R. Yu, H. M. Weng, Z. Fang, X. Dai, J. Mesot, H. Ding, and M. Shi, Nat. Commun. **5**, 5 (2014).

[18] C. Varma, Rev. Mod. Phys. **48**, 219 (1976).

[19] X. Y. Feng, J. Dai, C. H. Chung, and Q. Si, Phys. Rev. Lett. **111**, 016402 (2013).

[20] G. Li, Z. Xiang, F. Yu, T. Asaba, B. Lawson, P. Cai, C. Tinsman, A. Berkley, S. Wolgast, Y. S. Eo, D.-J. Kim, C. Kurdak, J. W. Allen, K. Sun, X. H. Chen, Y. Y. Wang, Z. Fisk, and L. Li, Science **346**, 1208 (2014).

[21] D. J. Kim, J. Xia, and Z. Fisk, Nat. Mater. **13**, 466 (2014).

[22] M. Dzero, K. Sun, V. Galitski, and P. Coleman, Phys. Rev. Lett. **104**, 106408 (2010).

[23] J. Jiang, S. Li, T. Zhang, Z. Sun, F. Chen, Z. R. Ye, M. Xu, Q. Q. Ge, S. Y. Tan, X. H. Niu, M. Xia, B. P. Xie, Y. F. Li, X. H. Chen, H. H. Wen, and D. L. Feng, Nat. Commun. **4**, 3010 (2013).

[24] S. Wolgast, Ç. Kurdak, K. Sun, J. W. Allen, D.-J. Kim, and Z. Fisk, Phys. Rev. B **88**, 180405 (2013).

[25] S. Rößler, T.-H. Jang, D.-J. Kim, L. H. Tjeng, Z. Fisk, F. Steglich, and S. Wirth, Proceedings of the National Academy of Sciences **111**, 4798 (2014).

[26] D. J. Kim, S. Thomas, T. Grant, J. Botimer, Z. Fisk, and J. Xia, Sci. Rep. **3**, 3150 (2013).

[27] J. Yong, Y. Jiang, D. Usanmaz, S. Curtarolo, X. Zhang, L. Li, X. Pan, J. Shin, I. Takeuchi, and R. L. Greene, Appl. Phys. Lett. **105**, 222403 (2014).

[28] Z. Yue, X. Wang, D. Wang, J. Wang, D. Culcer, and S. Dou, J. Phys. Soc. Jpn. **84**, 044717 (2015).

[29] F. Chen, C. Shang, Z. Jin, D. Zhao, Y. P. Wu, Z. J. Xiang, Z. C. Xia, A. F. Wang, X. G. Luo, T. Wu, and X. H. Chen, Phys. Rev. B **91**, 205133 (2015).

[30] Y. Luo, H. Chen, J. Dai, Z.-a. Xu, and J. D. Thompson, Phys. Rev. B **91**, 075130 (2015).

[31] N. Wakeham, Y. Q. Wang, Z. Fisk, F. Ronning, and J. D. Thompson, Phys. Rev. B **91**, 085107 (2015).

[32] N. Xu, C. E. Matt, E. Pomjakushina, X. Shi, R. S. Dhaka, N. C. Plumb, M. Radović, P. K. Biswas, D. Evtushinsky, V. Zabolotnyy, J. H. Dil, K. Conder, J. Mesot, H. Ding, and M. Shi, Phys. Rev. B **90**, 085148 (2014).

[33] W. T. Fuhrman, J. Leiner, P. Nikolić, G. E. Granroth, M. B. Stone, M. D. Lumsden, L. DeBeer-Schmitt, P. A. Alekseev, J. M. Mignot, S. M. Koohpayeh, P. Cottingham, W. A. Phelan, L. Schoop, T. M. McQueen, and C. Broholm, Phys. Rev.

Lett. **114**, 036401 (2015).

[34] W. Ruan, C. Ye, M. Guo, F. Chen, X. Chen, G.-M. Zhang, and Y. Wang, Phys. Rev. Lett. **112**, 136401 (2014).

[35] P. Syers, D. Kim, M. S. Fuhrer, and J. Paglione, Phys. Rev. Lett. **114**, 096601 (2015).

[36] B. S. Tan, Y.-T. Hsu, B. Zeng, M. C. Hatnean, N. Harrison, Z. Zhu, M. Hartstein, M. Kiourlappou, A. Srivastava, M. D. Johannes, T. P. Murphy, J.-H. Park, L. Balicas, G. G. Lonzarich, G. Balakrishnan, and S. E. Sebastian, Science **349**, 287 (2015).

[37] N. Xu, C. E. Matt, E. Pomjakushina, J. H. Dil, G. Landolt, J.-Z. Ma, X. Shi, R. S. Dhaka, N. C. Plumb, M. Radovic, V. N. Strocov, T. K. Kim, M. Hoesch, K. Conder, J. Mesot, H. Ding, and M. Shi, arXiv:1405.165

[38] M. Neupane, S.-Y. Xu, N. Alidoust, G. Bian, D. J. Kim, C. Liu, I. Belopolski, T. R. Chang, H. T. Jeng, T. Durakiewicz, H. Lin, A. Bansil, Z. Fisk, and M. Z. Hasan, Phys. Rev. Lett. **114**, 016403 (2015).

[39] E. Frantzeskakis, N. de Jong, J. X. Zhang, X. Zhang, Z. Li, C. L. Liang, Y. Wang, A. Varykhalov, Y. K. Huang, and M. S. Golden, Phys. Rev. B **90**, 235116 (2014).

[40] C.-J. Kang, J. D. Denlinger, J. W. Allen, C.-H. Min, F. Reinert, B. Y. Kang, B. K. Cho, J.-S. Kang, J. H. Shim, and B. I. Min, arXiv:1508.7212

[41] H. K. Mao, J. Xu, and P. M. Bell, J. Geophys. Res. **91**, 4673 (1986).

[42] V. A. Sidorov, N. N. Stepanov, O. B. Tsiok, L. G. Khvostantsev, I. A. Smirnov, M. M. Korsukova, and A. Tybulewicz, Sov. Phys. Solid State **33**, 720 (1991).

[43] T. Nanba, M. Tomikawa, Y. Mori, N. Shino, S. Imada, S. Suga, S. Kimura, and S.

Kunii, Phys. B: Cond. Matter **186–188**, 557 (1993).

Acknowledgements

The work in China wassupported by the NSF of China (Grant No. 91321207, 11427805, 11404384, 11174339, U1532267) and the Strategic Priority Research Program (B) of the ChineseAcademy of Sciences (Grant No. XDB07020300, XDB07020200). The works in the USA were supported by DARPA under agreement number FA8650-13-1-7374 and FAPESP 2013/2018-0.

†To whom correspondence should be addressed.
E-mail: llsun@iphy.ac.cn

Figure captions:

Figure 1(a) Resistance-Temperature (*R-T*)curves measured in pressure range 0.9-8.8 GPa, showing a remarkable pressure-induced resistance decrease over entire temperature range. The inset displays normalized *R-T* curves in the low temperature range, showing the upturns of the resistance measured at different pressures. (b) Selective *R-T* curves in the pressure range 10.5-17.6 GPa, displaying a dramatic change in resistance.(c) The *R-T* curves measured in pressure range 19.8-26.4 GPa, exhibiting a significant pressure-induced enhancement of non-metallic behavior. The inset shows the resistance plateaus (T*) in lower temperature at different pressures. (d) T* as a function of pressure. (e) The pressure dependence of the resistance obtained at different fixed temperatures, illustrating two critical pressures (P_{C1} and P_{C2}). (f) Hall coefficient (R_H) as a function of pressure for single crystal YbB_6 at 4K.

Figure 2 (a) X-ray diffraction patterns of YbB_6 collected at different pressures, showing that no structure phase transition occurs over entire pressure range investigated. (b) and (c) Pressure dependences of lattice parameter and volume of YbB_6, respectively.

Figure 3 (a) Phase diagram of pressure dependence of activation energy gap (ε_a, left axis) and temperature (right axis), as well as the summary of *dR/dT* as a function of temperature and pressure. The orange solid dots represent the activation gap. The acronyms TT-S and TNT-HP phase stand for the topologically trivial semiconducting state and topologically non-trivial high-pressure gapped phase, respectively. SM represents semimetallic state. The value of the ε_a in TT-S regime is scaled by 0.5 to fit the pressure dependence of *dR/dT*. (b)-(d) Temperature dependence of resistance measured at zero field and 7 T at fixed pressure. The insets illustrate the details for the measurements. The acronyms in the inset of Fig. 3b, I, V and H, stand for current, voltage and magnetic field, respectively.

Figure 4(a) X-ray absorption spectra (XAS) of Yb through the L_{III}-edge at different pressures. The dashed vertical lines indicate characteristic energy positions of L_{III}-edge peak for Yb^{2+} and Yb^{3+}, respectively. (b) XAS of Yb measured at ambient pressure and 28.2 GPa, after the background deduction. The light gray area and dark gray area represent the Yb^{2+} component and Yb^{3+}component, respectively. (c)

Pressure dependence of mean valence determined from XAS data.

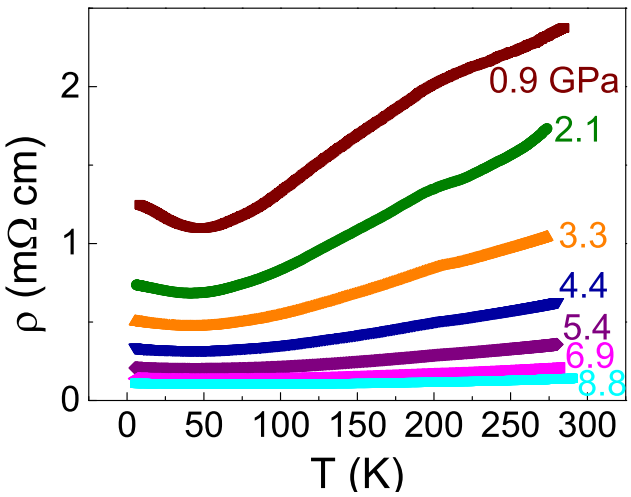

Figure 1 LB14790BR 10DEC2015

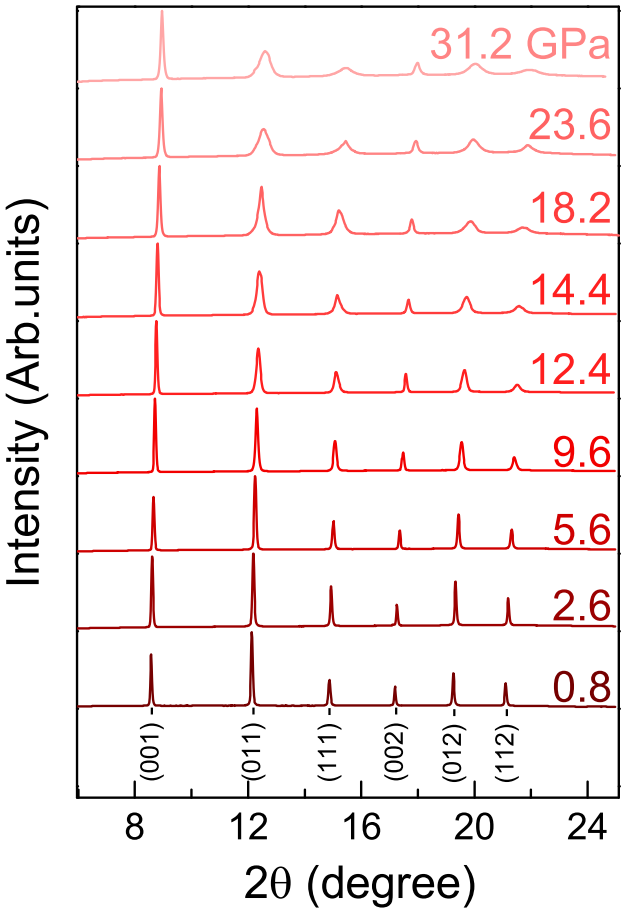

Figure 2 LB14790BR 10DEC2015

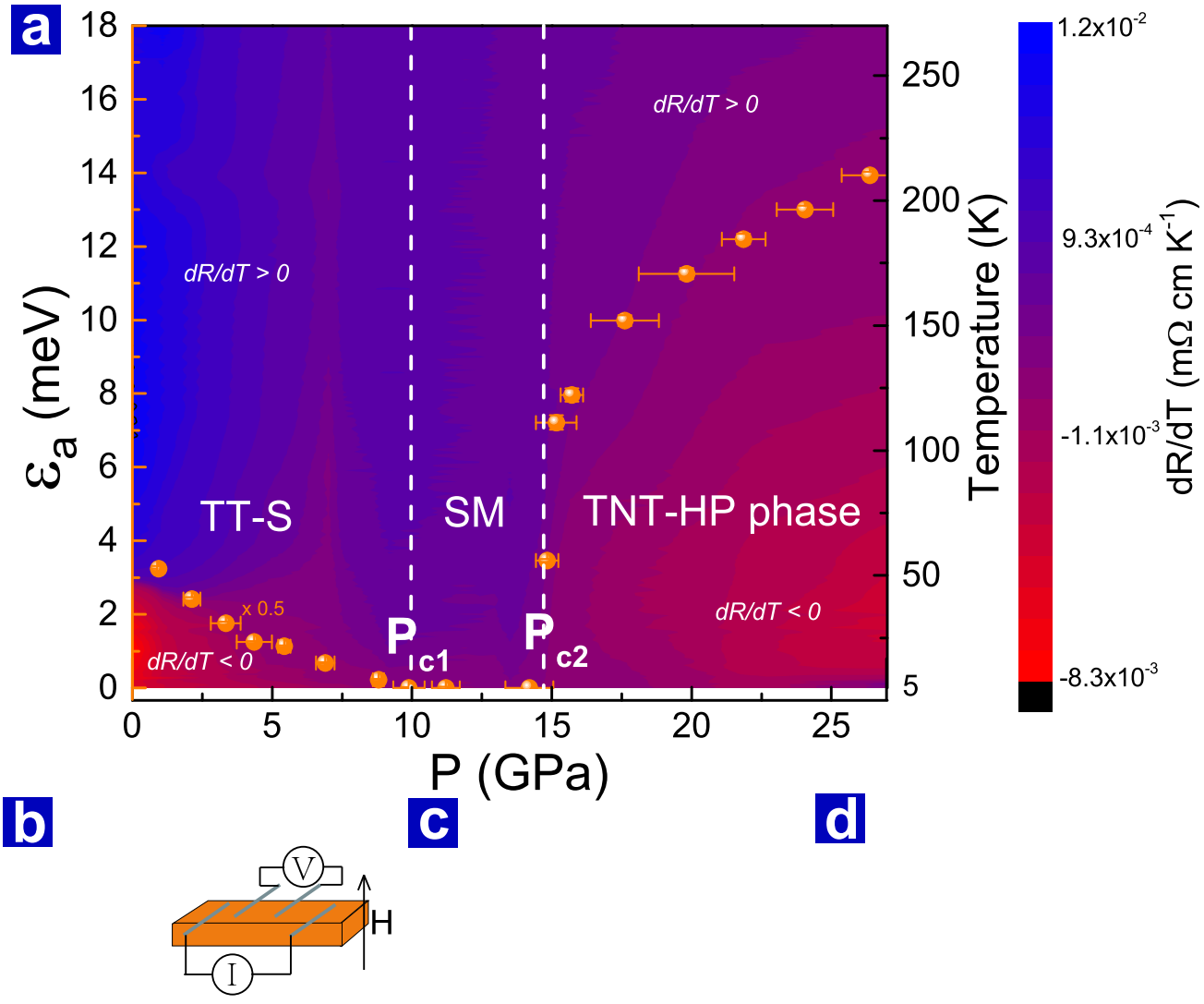

Figure 3 LB14790BR 10DEC2015

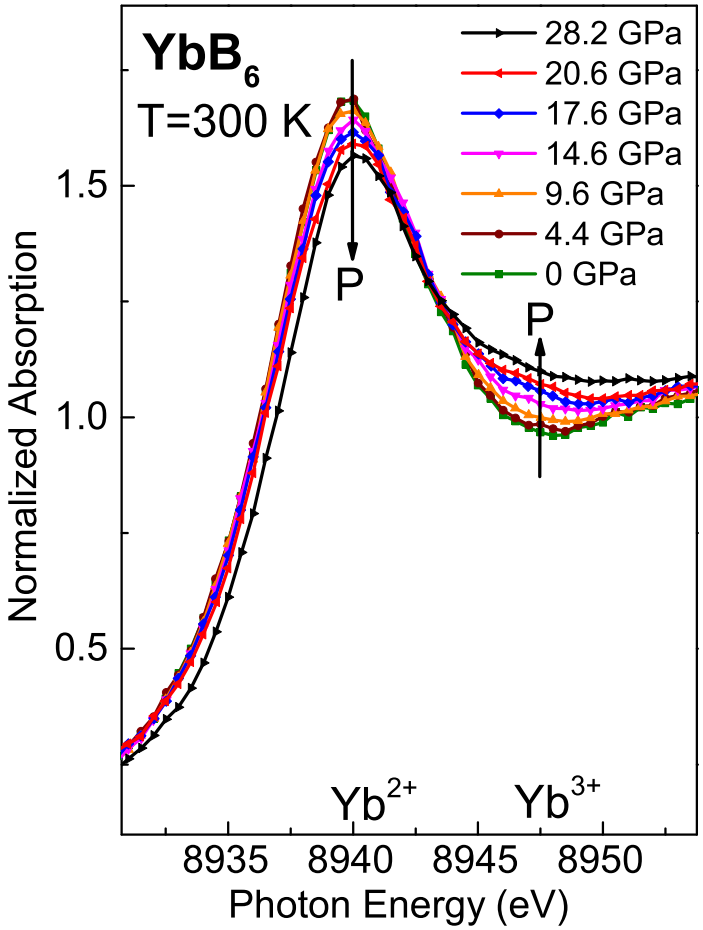

Figure 4 LB14790BR 10DEC2015